STAFF SUMMARY SHEET

	TO	ACTION	SIGNATURE (Surname), GRADE AND DATE		TO	ACTION	SIGNATURE (Surname), GRADE AND DATE
1	USAFA/ DFAN	sig	_Susan M Cummings_ HEAD 17 MAR 2014	6			
2	USAFA/ DFER	approve	_Kraus, Col 18 Mar 14_	7			
3	USAFA/ DFAN	action	(Author / Originator)	8			
4				9			
5				10			

SURNAME OF ACTION OFFICER AND GRADE	SYMBOL	PHONE	TYPIST'S INITIALS	SUSPENSE DATE
Kurt P. Rouser, Lt Col, USAF	Hq USAFA/DFAN	333-8489	kpr	20140321

SUBJECT	DATE
Clearance for Material for Public Release USAFA-DF-PA- 185	20140317

SUMMARY

1. PURPOSE. To provide security and policy review on the document at Tab 1 prior to release to the public.

2. BACKGROUND.

Authors: Connor Wiese, Michael McClearn, Giovanni Allevato, Richard Guttman and Kurt P. Rouser

Title: Passive Turbulence Generating Grid Arrangements in a Turbine Cascade Wind Tunnel

Circle one: Abstract   Tech Report   Journal Article   Speech   **Paper**   Presentation   Poster

Thesis/Dissertation   Book   Other: _____

Check all that apply (For Communications Purposes):

[] CRADA (Cooperative Research and Development Agreement) exists

[] Photo/ Video Opportunities   [] STEM-outreach Related   [] New Invention/ Discovery/ Patent

Description: Paper for 2014 American Institute of Aeronautics and Astronautics (AIAA) Region V Student Conference
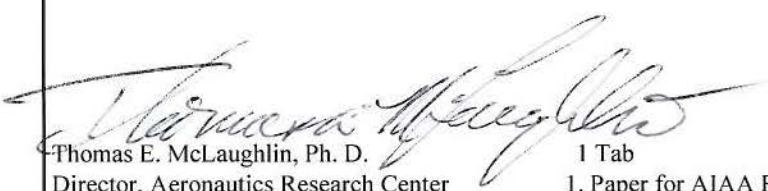
Release Information: AIAA Region V Student Conference, Minneapolis, MN, 2-4 Apr 2014

Previous Clearance information: None

Recommended Distribution Statement: Distribution A, Approved for Public Release, Distribution Unlimited.

3. DISCUSSION. N/A

4. RECOMMENDATION. Sign coord block above indicating document is suitable for public release. Suitability is based soley on the document being unclassified, not jeopardizig DoD interests, and accurately portraying official party.

Thomas E. McLaughlin, Ph. D.   1 Tab
Director, Aeronautics Research Center   1. Paper for AIAA Region V Student Conference

---

AF IMT 1768, 19840901, V5   PREVIOUS EDITION WILL BE USED.

Passive Turbulence Generating Grid Arrangements in a Turbine Cascade Wind Tunnel

Connor J. Wiese[*], Michael J. McClearn[†], Giovanni Allevato[‡], and Richard T. Guttman III[§]
United States Air Force Academy, USAFA, CO, 80841

and

Kurt P. Rouser[¶]
United States Air Force Academy, USAFA, CO, 80841

Turbine cascade wind tunnels simulate Reynolds number and turbulence for the examination of flow phenomena such as boundary layer separation on the trailing portion of low pressure turbine blades. Axial chord-based Reynolds numbers considered in this study were 50k and 100k. Various passive, square-bar turbulence generating grid arrangements were explored to simulate turbulence in a turbine cascade test-section inlet, including two grid orientations: perpendicular to the inlet flow and parallel to the turbine cascade. A novel T-Bar turbulence grid configuration oriented parallel to the cascade was shown to produce better test section inlet flowfield uniformity than that produced by a perpendicular mesh grid. Improved periodicity in blade-to-blade surface pressure coefficient profiles was also observed with the parallel T-Bar grid.

Nomenclature

B	=	bias error	S	=	suction surface length
B_1	=	inlet camber angle	Tu	=	free stream turbulence intensity
B_2	=	exit camber angle	T	=	static temperature
C	=	true chord	U	=	total error
C_p	=	blade surface pressure coefficient	$\bar{V}$	=	mean velocity
C_x	=	axial chord length	V_i	=	free stream velocity (from dynamic pressure)
d	=	grid element diameter			
N	=	number of samples	V_l	=	free stream velocity (from hotwire)
m	=	mesh width	V_N	=	normalized inlet velocity
P	=	precision error	x	=	upstream grid location
P_x	=	static pressure	y	=	pitchwise location
P_t	=	total pressure	ρ	=	flow density
$P_{t\infty}$	=	free stream total pressure	σ_V	=	root mean square of free stream velocity
p	=	pitchwise spacing			
q	=	inlet dynamic pressure	μ	=	flow viscosity
Re_{Cx}	=	axial chord based Reynolds number			

I. Introduction and Background

Turbine Cascade Wind Tunnels (CWT) are similar to conventional wind tunnels except the test section of interest is in a corner. Figure 1 shows the United States Air Force Academy (USAFA) closed-loop CWT. Turbine cascade facilities are used to simulate turbine operating conditions for the study of flow phenomena such as

---

[*] Cadet First Class, Department of Aeronautics, PO Box 3365, Student Member.
[†] Cadet First Class, Department of Aeronautics, PO Box 4180, Student Member.
[‡] Cadet First Class, Department of Aeronautics, PO Box 1465, Student Member.
[§] Cadet First Class, Department of Aeronautics, PO Box 1454, Student Member.
[¶] Assistant Professor, Department of Aeronautics, 2354 Fairchild Drive, Associate Fellow.

boundary layer separation over the trailing portion of a turbine suction surface. In addition to Reynolds number, turbulence must also be simulated because turbine performance is sensitive to both. Turbines are susceptible to adverse flow effects at low Reynolds numbers and low turbulence intensities.
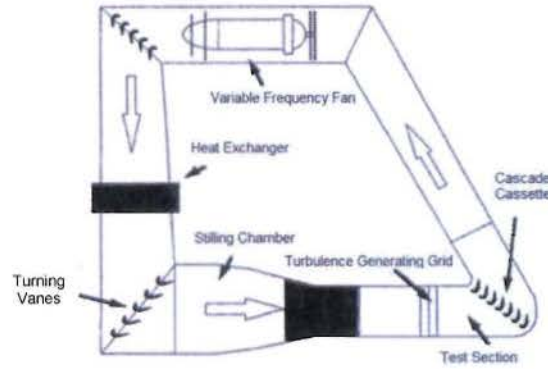
Figure 1. Schematic of USAFA Cascade Wind Tunnel[1]

A. Turbulence Generation

An extensive study by P.E. Roach[2] characterized turbulence generating grids in conventional wind tunnels. Figure 2 shows the relationship between turbulence intensity (Tu) and upstream grid location, x, normalized by diameter, d, of grid elements. Experimental turbulence intensity is defined in Eq. 1, and Roach observed the correlation shown in Eq. 2. Turbulence is generated by vortex shedding as flow passes through a grid, as shown in Fig. 1. Roach found that the minimum upstream grid location, normalized by the grid mesh width, m, is 10, ensuring that vortices are fully mixed upstream of the test article.
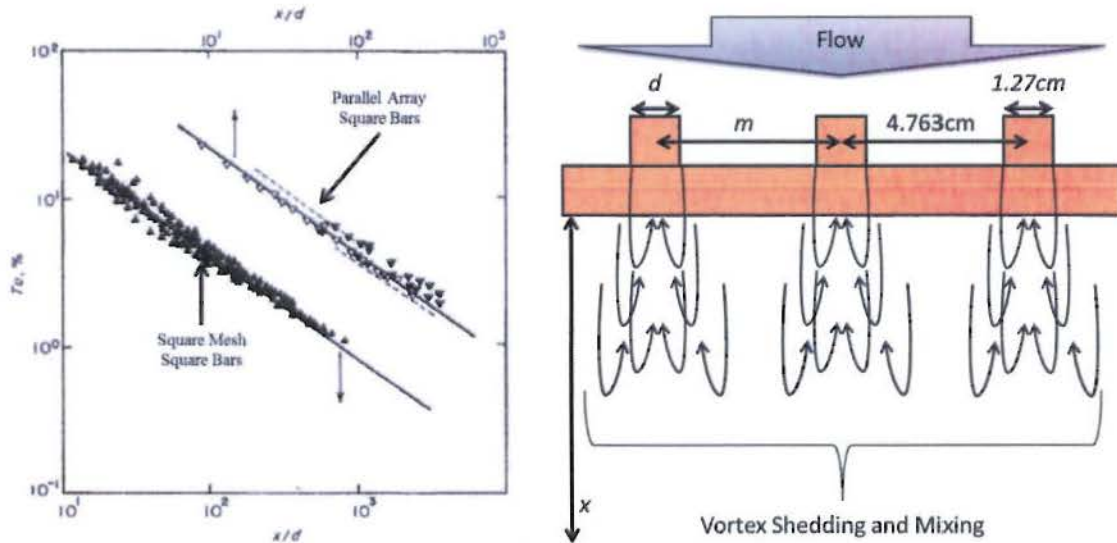
Figure 2. Turbulence Decay as a Function of x/d (left)[2] and Generation of Turbulence by Grids (right)

$$Tu = \frac{\sigma_V}{\bar{V}} \tag{1}$$

$$Tu = 1.13(x/d)^{-(5/7)} \tag{2}$$

2

B. Turbine Cascade Theory

Baughn, et al.[3], showed that two-dimensional (2-D) turbine blade interactions can be simulated with a cassette of high aspect ratio blades. Figure 3 shows the relation between flow effects in a three-dimensional (3-D) turbine and a cascade blade. Cascade blades represent a mid-span airfoil of a 3-D turbine extruded spanwise so that the blade wake and surface boundary layers can be isolated from the other 3-D effects, as tabulated in Fig. 3. Furthermore, by evaluating only the middle third span of the blade, the ceiling and floor effects in the tunnel can be mitigated. A CWT test section inlet must have uniform flowfield properties. The inlet conditions of interest upstream of the cascade include velocity and turbulence intensity.
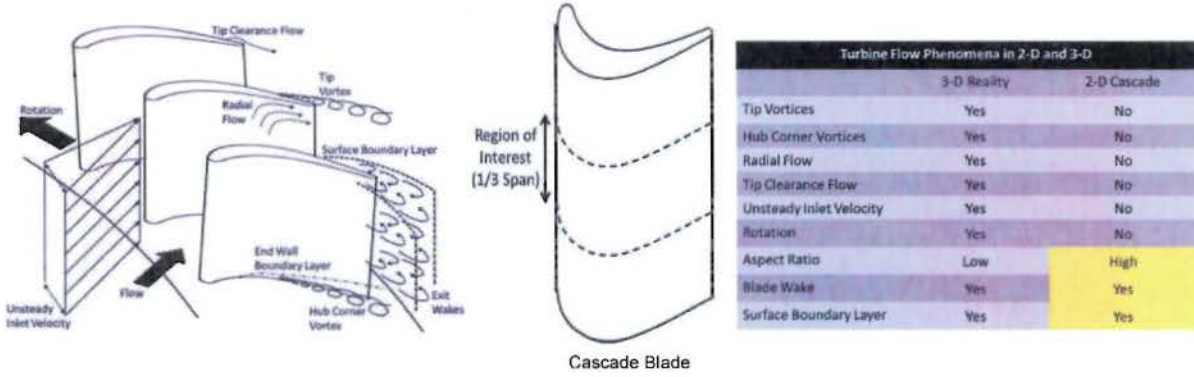

Cascade Blade

Turbine Flow Phenomena in 2-D and 3-D		
	3-D Reality	2-D Cascade
Tip Vortices	Yes	No
Hub Corner Vortices	Yes	No
Radial Flow	Yes	No
Tip Clearance Flow	Yes	No
Unsteady Inlet Velocity	Yes	No
Rotation	Yes	No
Aspect Ratio	Low	High
Blade Wake	Yes	Yes
Surface Boundary Layer	Yes	Yes

Figure 3. Relation between 3-D Turbine and 2-D Simulation

CWT blade surface pressure coefficient (C_p) is useful to evaluate turbine flowfields. Butler, et al.[4], defined C_p as shown in Eq. 3; however, in this current study C_p is given by Eq. 4, such that local dynamic pressure is normalized by the inlet dynamic pressure. Butler, et al.[4], previously showed C_p results from the USAFA CWT as shown in Fig. 4, using a turbulence generating grid placed upstream of the turbine cascade and oriented perpendicular to the flow.
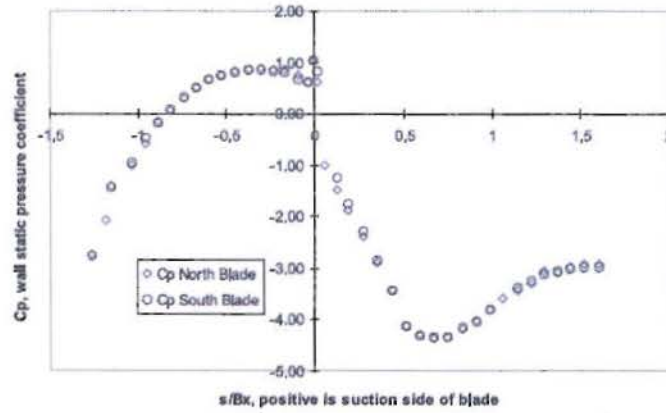

s/Bx, positive is suction side of blade

Figure 4. Example Pressure Coefficient Results[4]

$$C_p = \frac{P_{Slocal} - P_{Sin}}{q_{in}} \tag{3}$$

$$C_P = \frac{P_{t\infty} - P_s}{q_f} \tag{4}$$

C. Turbine Airfoil Theory

The underside of the turbine airfoil as shown in Fig. 5 is the pressure surface, and the upper side is the suction surface. The suction surface length (S) is defined as the distance along the suction surface from the leading edge to the trailing edge, and axial chord length (C_x) is the straight line distance from the leading to trailing edge.

Axial chord-based Reynolds number (Re_{Cx}) is defined in Eq. 5, with ρ as flow density, V_α as inlet velocity, and μ is viscosity. At low Reynolds numbers, flow is laminar, and large turning angles associated with low pressure turbines (LPTs) cause an adverse pressure gradient over the trailing portion of the suction surface. Boundary layer separation may occur because the flow does not have enough momentum to stay attached. Separation is affected by the inlet turbulence intensity and the Reynolds number such that separation is more pronounced at both lower Reynolds numbers and turbulence intensities.
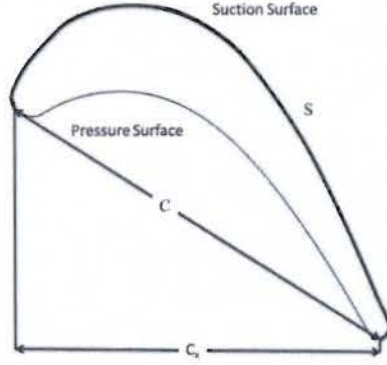
Figure 5. Turbine Airfoil Nomenclature

$$Re_{C_x} = \frac{\rho V C_x}{\mu} \tag{5}$$

D. Objectives

The objective of this study was to evaluate various turbulence generating grid configurations in a CWT. Two grids were studied at three upstream locations with $Re = 50k$ and $Re = 100k$, one grid oriented perpendicular to the flow and the other parallel to the turbine cascade. The grids were evaluated based on turbulence intensity and inlet velocity uniformity. Furthermore, C_p results show the sensitivity of turbine blade flowfields to grid configuration.

II. Set-up and Procedure

A. Facility

The USAFA CWT shown in Fig. 1 is driven by a variable-frequency, variable-pitch fan adjusted to achieve desired Re_{Cx} within the test section. The heat exchanger ensures thermal equilibrium such that the temperature inside the test section is adjusted to match the ambient temperature by regulating cooling water flow rate through heat exchanger piping. The stilling chamber ensures that air flow is straight and steady. Air flow passes through the turbulence grid, installed at an upstream distance to generate desired turbulence intensity.

Figure 6 shows Langston blades installed in the USAFA CWT test section, spaced equally pitchwise to approximate the arrangement in an actual turbine. The center blade is the test article, with surface measurements being taken on each adjacent blade. A variable tail board is located downstream of the cassette, and can be adjusted to change the exit cross-sectional area. Adjustment of the variable tail board affects the flow upstream of the cassette and thus affects periodicity. The USAFA CWT can utilize both perpendicular and parallel oriented grids. Grid distance from the test section is measured in terms of x/d, from the center test article to the middle of the grid.
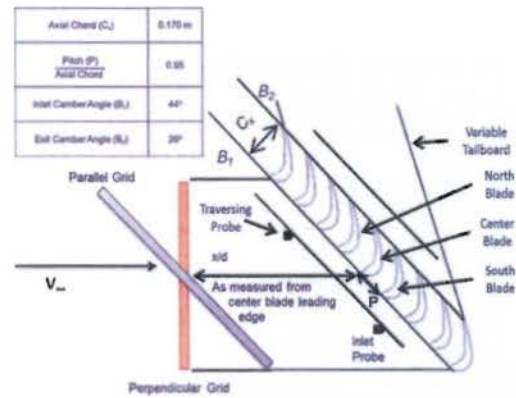
4

Axial Chord (C_x)	0.170 m
$\dfrac{\text{Pitch (P)}}{\text{Axial Chord}}$	0.95
Inlet Camber Angle (β_1)	44°
Exit Camber Angle (β_2)	20°

Figure 6. USAFA CWT Test Section Schematic

The north and south blades adjacent to the center blade each contain 40 surface pressure taps, allowing pressure coefficients to be determined along the blade suction and pressure surfaces. Pressure taps are instrumented with 20" of H_2O and 10" of H_2O pressure transducers connected to PSI 8400, which transfers data to a data acquistion computer located next to the tunnel. Two probe configurations are shown in Fig. 6 for inlet traverse measurements. The fixed inlet probe contains three co-located measurement devices: a thermocouple, a pitot-static probe, and a Kiel probe, while the traversing probe contains a Kiel probe and a hotwire anemometer. The traversing Kiel probe is differenced against the static pressure collected by the fixed inlet probe. The entire probe suite is instrumented with three, 1-torr Baratron pressure transducers. Additionally, the ambient temperature and pressure readings were collected using a Heise barometer and thermometer.

B. Procedures

For a pressure coefficient test, the first step was to properly orient and secure the desired turbulence generating grid. The turbulence generating grids utilized in this study are shown in Fig. 7. These grids are a perpendicular mesh grid (PMG) and a parallel T-bar grid (PTG). The T-Bar grid was constructed using discrete, non-overlapping horizontal elements, mounted on a parallel array of square bars; so that the grid area projected on the flow field is equal to the perpendicular mesh grid. The fan speed was adjusted so that the corresponding velocity yielded the desired Reynolds number. Once the desired temperature and Reynolds numbers were achieved, data was collected using the PSI 8400 system.
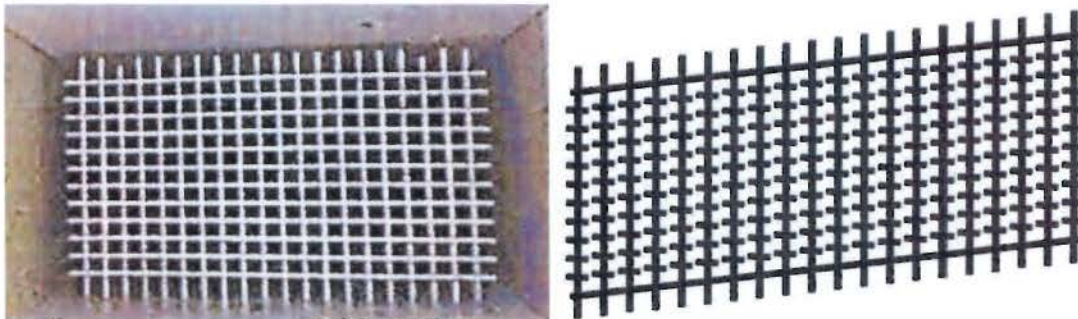

Figure 7. Perpendicular Mesh Grid (left), and Parallel T-Bar Grid (Right)

The air velocity was measured using a hotwire calibrated in-situ. Every run required a hot wire calibration which consisted of increasing the Re_{Cx} in increments of 10,000, starting at 15,000 and going to 125,000. These data files were then graphed and fitted with a 4th order polynomial curve.

TunnelVision was used for traverse control and LabView for data collection. Velocity, pressure and temperature data were collected at 1200Hz for 40.96 seconds at each pitchwise location.

III. Results and Discussion

A. Inlet Turbulence and Velocity Profiles

Figure 8 shows the inlet turbulence intensity (Tu) and normalized inlet velocity (V_N) profiles for clean tunnel, PMG, and TBG runs at an axial chord-based Reynolds number of 100k. The grids were located at an x/d location of 164. At these conditions, the clean tunnel inlet profiles exhibit good uniformity across the inlet. The PMG exhibits uniform turbulence intensity. However, at the inboard section of the traverse, there is a slight increase in turbulence intensity due to the decreasing grid x/d across the inboard half of the PMG, pitchwise-relative to the cascade. Additionally, the normalized velocity profile exhibits poor uniformity when compared to the clean tunnel configuration. The TBG turbulence intensity profile remains constant across the inlet due to the constant x/d pitchwise-relative to the cascade. It is apparent that at these conditions, the TBG produces a more uniform inlet than that of the PMG.

$$V_N = \frac{v_l}{v_i} \qquad (6)$$

Figure 9 shows the inlet turbulence intensity and normalized inlet velocity profiles for PMG and TBG runs at an axial chord-based Reynolds number of 50k, and a grid x/d of 164. With the decrease in axial chord-based Reynolds number, the change in turbulence intensity characteristics were minimal, and were consistent with Roach[2], such that turbulence intensity was independent of free-stream velocity. Unlike the $Re_{Cx} = 100k$ run, both grids exhibit uniform normalized velocity profiles across the inlet, except at pitchwise locations less than $y/p = -1.8$. The turbulence intensity profile generated by the TBG is constant across the inlet, similar to the $Re_{Cx} = 100k$ run. As Reynolds number decreased the TBG provided a more uniform inlet than that of the PMG.
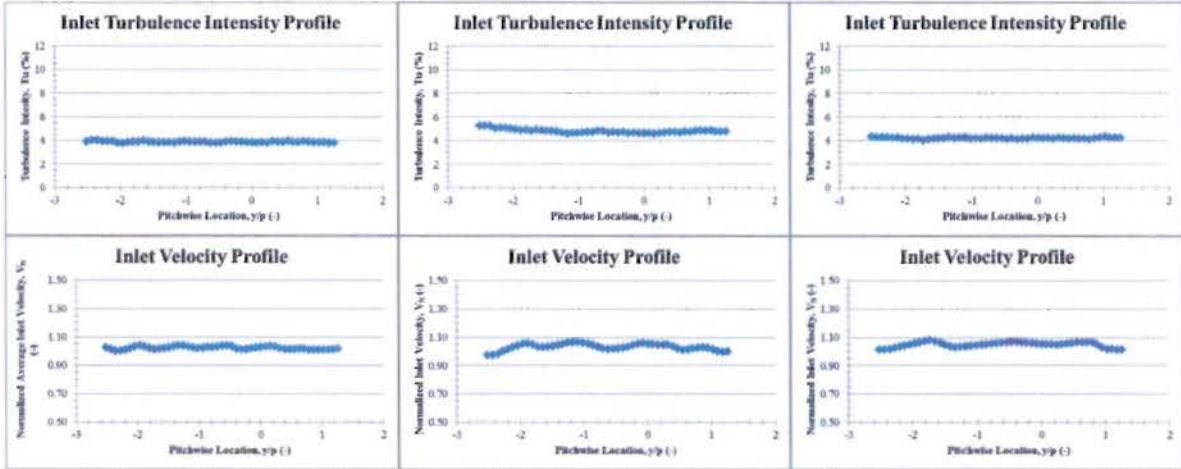

Figure 8. *Re* = 100k Inlet Profiles for Clean Tunnel (Left), PMG at *x/d* = 164 (Center), and TBG at *x/d* = 164 (Right)
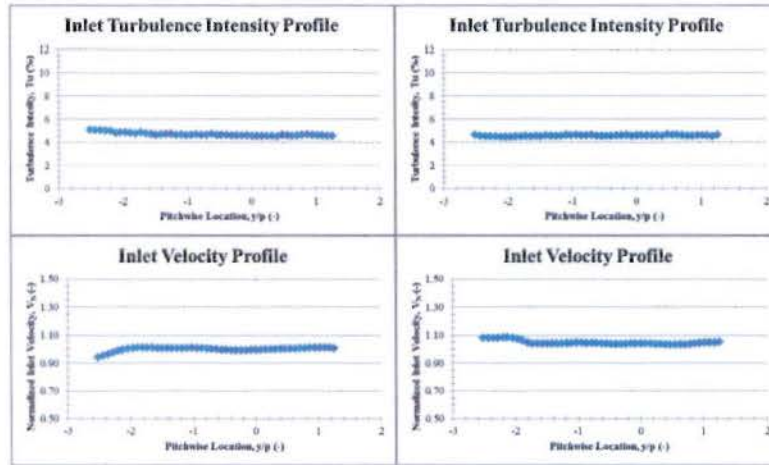
Figure 9. *Re* = 50k Inlet Profiles for PMG (Left) and TBG (Right) at *x/d* = 164

Figures 10 and 11 show the effect of decreasing grid *x/d* on inlet turbulence intensity and normalized inlet velocity at Re_{Cx} = 100k. As noted at a grid *x/d* of 164, the PMG turbulence intensity increases on the inboard half of the grid, pitchwise-relative to the cascade, while the TBG exhibits relatively constant turbulence intensity pitchwise relative to the cascade. Additionally, like the *x/d* = 164 condition, the TBG exhibits better inlet velocity uniformity than the PMG. At an *x/d* location of 64, the grids exhibited similar trends. However, the effect of decreasing *x/d* pitchwise-relative to the grid was more pronounced for the PMG because the effect of non-constant *x/d* on turbulence intensity is more pronounced at smaller *x/d* locations. The PMG inlet velocity profile, however, was more uniform at *x/d* = 64 than at *x/d* = 164. The TBG exhibited more uniform turbulence intensity and velocity profiles than the PMG. However, at an *x/d* of 64, both turbulence intensity and inlet velocity increased with outboard pitchwise location, relative to the cascade. This trend is likely due to the TBG not being mounted perfectly parallel to the cascade. However, when compared to the PMG, the TBG produces more favorable inlet profiles. Additionally, at no time was the tunnel velocity expected to exceed 15 m/s, correlating to a ~M=0.0132, well within the incompressible flow regime.
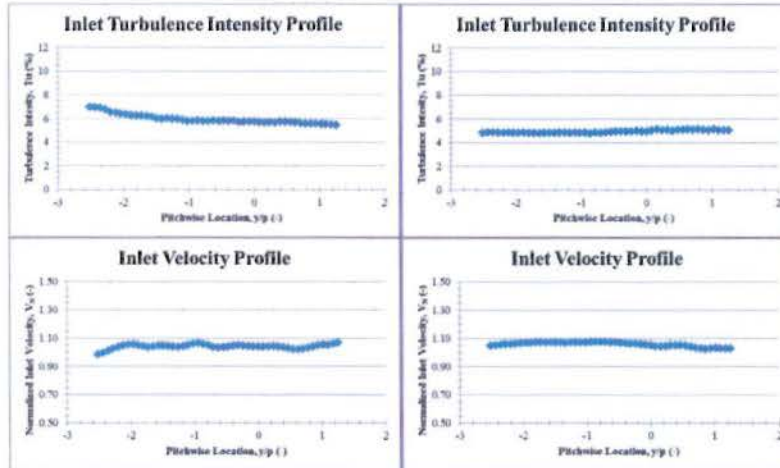

Figure 10. *Re* = 100k Inlet Profiles for PMG (Left) and TBG (Right) at *x/d* = 104
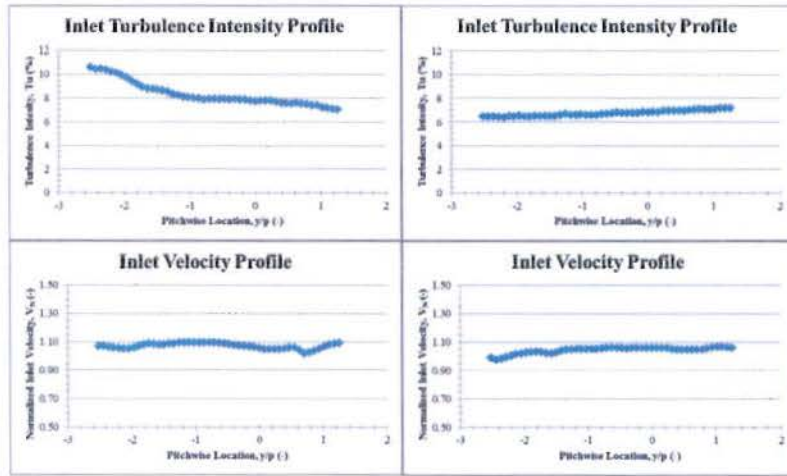
7

Figure 11. *Re* = 100k Inlet Profiles for PMG (Left) and TBG (Right) at *x/d* = 64

B. Surface Pressure Coefficient Analysis

Figure 12 compares C_p results for the clean tunnel, perpendicular mesh, and parallel T-bar grids yields some specific trends. At a higher inlet velocities, only minimal turbulence is required to maintain flow attachment. The clean tunnel profile, as seen in the left most picture in Fig. 12, has a turbulence intensity of approximately 4%. The perpendicular mesh (center) and parallel T-bar (right) have only fractional increases in turbulence. Figure 12 shows that all three configurations have a similar level of periodicity. The primary difference between the three configurations is the difference in suction surface peak. The perpendicular mesh generates the greatest magnitude but when comparing all three, the parallel T-bar looks most similar to the clean tunnel.
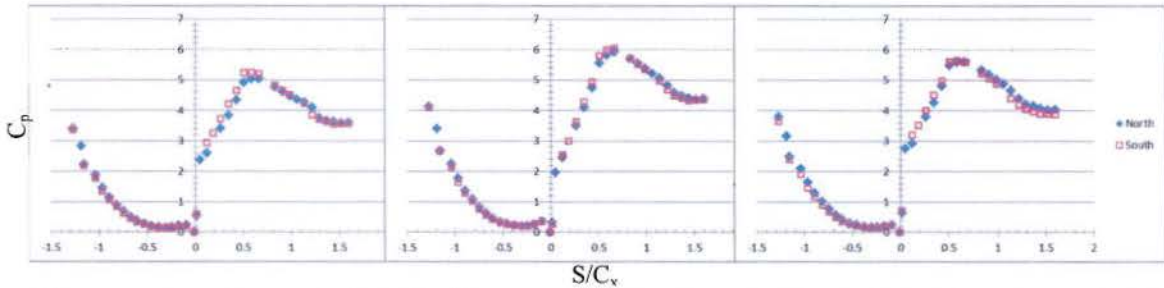

Figure 12. Clean Tunnel (Left), PMG (Center), and TBG (Right) C$_p$ Results at *Re* = 100k and *x/d* = 164

Figure 13 shows results for the perpendicular mesh and parallel T-bar grid configurations at a *Re* = 50k. The suction surface peak for both cases drops from the 100k values, but there is still enough flow momentum to prevent full separation. This leads to the conclusion that Reynolds number is not the most important factor for C_p.
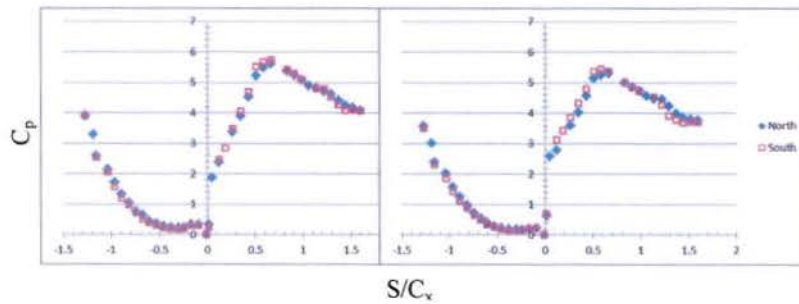

Figure 13. PMG (Left) and TBG (Right) C$_p$ results at *Re* = 50k and *x/d* =164

Figure 14 shows the same configurations for *Re* = 100k and a smaller x/d value which increases the level of turbulence seen at the test section. Figure 14 has nearly the same level of periodicity as Fig. 13, but shows elevated suction surface peaks. The higher turbulence intensities result in more acceleration over the suction surface of the blade.
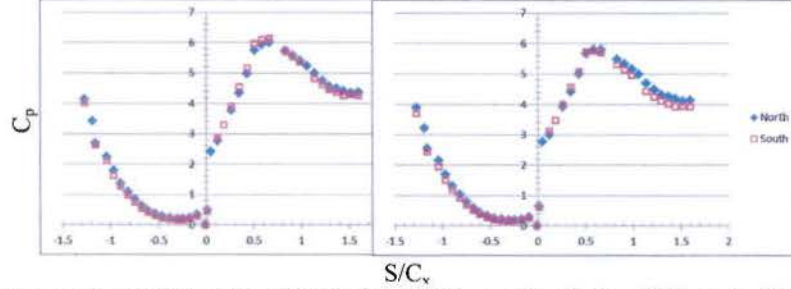

Figure 14. PMG (Left) and TBG (Right) C$_p$ results at *Re* = 100k and x/d = 104

Figure 15 again has the same configurations but at the closest x/d value. As seen previously, there is no apparent difference in periodicity, but another rise in suction surface peak value suggesting that increasing turbulence intensity affects the local acceleration over the suction surface.
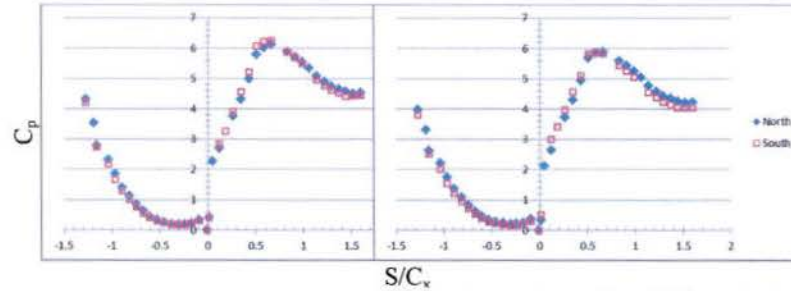

Figure 15. PMG (Left) and TBG (Right) C$_p$ results at *Re* = 100k and x/d = 64

The C$_p$ results show that Reynolds numbers studied do not cause much change but varying levels of turbulence affect the local flow acceleration over the suction surface. These results match those of Butler, et al.[4] with regards to differential magnitude between pressure and suction surfaces.

C. Uncertainty Analysis

An uncertainty analysis was conducted on turbulence intensity and Reynolds number. Repeatability runs were conducted with the PMG located at an x/d location of 164. Eight repeatability runs were conducted at 50k. Equations 7-9 outline the uncertainty process, where partial derivatives are also known as influence coefficients. Table 1 shows Reynolds number uncertainty with a target Reynolds number of 50k. *Re* = 50k exhibited the most uncertainty. Table 2 shows turbulence intensity uncertainty at a target Reynolds number of 50k. For turbulence intensity uncertainty, the traversing hotwire was removed and a hotwire was added to the fixed inlet probe. Like Reynolds number uncertainty, the greatest turbulence uncertainty was expected to be at the lower velocities. Reynolds number and turbulence intensity uncertainty were less than 5%.

$$B_G = \sqrt{\left(\frac{\partial G}{\partial x_1} B_1\right)^2 + \left(\frac{\partial G}{\partial x_2} B_2\right)^2 + \cdots + \left(\frac{\partial G}{\partial x_n} B_n\right)^2} \tag{7}$$

$$P_G = \sqrt{\left(\frac{\partial G}{\partial x_1} P_1\right)^2 + \left(\frac{\partial G}{\partial x_2} P_2\right)^2 + \cdots + \left(\frac{\partial G}{\partial x_n} P_n\right)^2} \tag{8}$$

$$U_G = \sqrt{B_G^2 + P_G^2} \tag{9}$$

9

Table 1. Reynolds Number Uncertainty for *Re* = 50k, *x/d* = 164

		Average	Influence Coefficient	B		P		U
P_t	Torr	0.1039	42.64208608	5%		2.1%		
P_{amb}	Torr	588.14	42.64208608	0.1%		0.18%		
q	Torr	0.1203	208431.7028	4%		0.41%		
T	K	298.41	-213.4711329	0.59%		0.11%		
Re		50855						2.2%

Table 2. Turbulence Intensity Uncertainty for *Re* = 50k, *x/d* = 164

		Average	Influence Coefficient	P		U
V	m/s	5.41	0.007437276	0.48%		
σ_V	m/s	0.22	0.184796322	2.09%		
Tu		4.02%				0.1%

IV. Conclusion

This study shows that the TBG produces a more uniform inlet than the PMG at similar test conditions. Additionally, the TBG surface pressure coefficients match clean tunnel data better than the PMG. Therefore, the authors suggest that future CWT studies be conducted with grids mounted parallel to the cascade. Future studies are recommended to evaluate turbulence length scales and turbulence isotropy for parallel T-Bar grids, like that utilized in this study.

Acknowledgements

References

[1] Van Treuren K. W., Byerley A. R., Simon T., von Koller M., Baughn J. W., Rivir R., "Measurements in a turbine cascade flow under ultra low Reynolds number conditions", ASME TURBOEXPO, 2001.

[2] Roach, P.E., "The Generation of Nearly Isotropic Turbulence by Means of Grids," Heat and Fluid Flow, Vol. 8, No. 2, June 1967, pp.82-91.

[3] Baughn, J. W., Byerley, A. R., Butler, R. J., and Rivir, R. B., "An Experimental Investigation of Heat Transfer, Transition and Separation on Turbine Blades at Low Reynolds Number and High Turbulence Intensity," *1995 International Mechanical Engineering Congress and Exposition.* Aero Propulsion and Power Directorate, Air Force Materiel Command. 1995 pp.1-14.

[4] Butler, Robert. J., Byerley, A. R., VanTreuren, K. W., Baughn, J. W., "The effect of turbulence intensity and length scales on low-pressure turbine blade aerodynamics," International Journal of Heat and Fluid Flow, Vol. 22, 2001, pp.123-133.